SCIENTIFIC REPORTS

OPEN

SUBJECT AREAS:
ELECTRONIC MATERIALS AND DEVICES
ELECTROCHEMISTRY
MATERIALS CHEMISTRY
CHEMICAL PHYSICS

Received
12 January 2012

Accepted
7 March 2012

Published
21 March 2012

Correspondence and requests for materials should be addressed to Z.P.S. (shaozp@njut.edu.cn) or Z.H.Z. (z.zhu@uq.edu.au)

Hierarchical CO_2-protective shell for highly efficient oxygen reduction reaction

Wei Zhou[1], Fengli Liang[1], Zongping Shao[2] & Zhonghua Zhu[1]

[1]Division of Chemical Engineering, The University of Queensland, Brisbane, Queensland 4072, Australia, [2]State Key Laboratory of Materials-Oriented Chemical Engineering, College of Chemistry & Chemical Engineering, Nanjing University of Technology, No.5 Xin Mofan Road, Nanjing 210009, PR China.

The widespread application of intermediate-temperature solid oxide fuel cells is mainly being hurdled by the cathode's low efficiency on oxygen reduction reaction and poor resistance to carbon dioxide impurity. Here we report the fabrication of a hierarchical shell-covered porous cathode through infiltration followed by microwave plasma treatment. The hierarchical shell consists of a dense thin-film substrate with cones on the top of the substrate, leading to a three-dimensional (3D) heterostructured electrode. The shell allows the cathode working stably in CO_2-containing air, and significantly improving the cathode's oxygen reduction reactivity with an area specific resistance of ~0.13 Ωcm^2 at 575°C. The method is also suitable for fabricating functional shell on the irregularly shaped substrate in various applications.

Lowering the operating temperature of solid oxide fuel cells (SOFCs) to intermediate temperature (IT, 500–700°C) has become a hot research point in commercialization of this charming technique in the past decades[1–3]. Low cost materials can be used and system is more reliable at reduced temperatures, opening great potential for the development of miniaturized SOFCs for portable power supply, thus the market of the SOFCs can be extended from big plants to every family[4].

The oxygen reduction reaction (ORR) on the cathode is the sluggish process throughout the whole fuel cell reaction when the temperature is reduced to <700°C[5–8], therefore development of highly efficient and stable cathode for SOFCs is the main task at the intermediate temperature region. The mixed ionic and electronic conducting (MIEC) oxides are the promising alternatives to replace the traditional high temperature cathode lanthanum strontium manganate (LSM), because oxygen reduction sites can be extended from three-phase boundary (TPB) to the whole surface of the cathode when the ionic conductivity is high enough[9].

Oxygen defects in the MIEC oxides are the passes for oxygen ions transportation. The demand of high oxygen ionic transport property of the cathode stimulates a growing interest in perovskite oxides with ABO_3 molecular formula structure, because the perovskites oxides are capable of accommodating remarkable oxygen defects[10].

In our previous study, a benchmark cathode-$Ba_{0.5}Sr_{0.5}Co_{0.8}Fe_{0.2}O_{3-\delta}$ (BSCF) has been developed, which shows surprising high oxygen reduction reactivity reflected by its low area specific resistance (ASR<0.15 Ω cm^2) at 600°C[11]. Unlike typical cathodes, the A-site cation of BSCF perovskite is an alkaline-earth species rather than a rare-earth element[11]. Consequently, we developed other two cathodes with A-site cations fully occupied by strontium, i.e. $SrNb_{0.1}Co_{0.9}O_{3-\delta}$ (SNC) and $SrSc_{0.2}Co_{0.8}O_{3-\delta}$ (SSC), which show comparable performance with BSCF[12,13]. The enhancement of ORR on these cathodes is related to alkaline-earth species which may increase the number of oxygen defects in the oxides, thus improving their reactivity. However, the perovskites containing alkaline-earth species are susceptible to CO_2 attack when temperature is decreased to the IT region[14–18]. The ASRs of BSCF and SSC cathodes increase by ~20 and ~12 times after introduction of 10 vol% CO_2 into air at 600°C for only 5 mins (Supplementary information, Fig S1).

The CO_2 poisoning effect is related to the basic property of the cathode surface[19]. The more basic the surface of perovskite is, the more likely it would be poisoned by CO_2. The metal oxides that have a very weak Madelung constant, such as BaO and SrO, can donate electrons more easily and thus have more basic surfaces. On the other hand, the presence of surface defects can also modify O basicity. Oxygen vacancies normally increase the individual O basicity. Decreasing the basicity of perovskite may improve the resistivity of perovskite to CO_2, but it also decreases the ORR activity of cathode. This is a trade-off between high oxygen reduction reactivity by using alkaline-earth species-containing cathode and high stability in CO_2 containing atmosphere.

Here we demonstrate a novel method to fabricate a CO_2-protective shell on BSCF cathode using infiltration followed by microwave plasma treatment. The shell can be made into a hierarchical structure consisting of a dense thin film $La_2NiO_{4+\delta}$ (LN) substrate and LN cones growing on the substrate. The shell allows the cathode working

stably in 10 vol% CO_2-containing air at 600°C, and significantly reduces the ASR of BSCF to ~0.13 Ω cm² at 575°C.

Results

Selection of shell material. We use LN as the shell material, because it is a mixed ionic and electronic conductor (MIEC) with resistivity to CO_2. To show LN's resistivity to CO_2, we treated the LN powders in 10 vol% CO_2-containing air for 1 h at 600°C. The treated LN powders were tested by Fourier transform infrared (FT-IR) spectroscopy (Supplementary information, Fig S2), which is a very sensitive technique to detect small quantities of CO_3^{2-}[20]. No characteristic peak belonging to CO_3^{2-} can be detected. Furthermore, the effect on the electrochemical performance of the LN cathode is negligible after introduction of 10 vol% CO_2 into air (Supplementary information, Fig S3). The CO_2 proof property of LN is likely due to the absence of alkaline-earth species and oxygen defects.

Even though LN is a MIEC, it is unsuitable as bulk cathode material for SOFC due to the anisotropic conduction of oxygen ions causing the low oxygen reduction reactivity of polycrystalline LN cathode at IT region. The ASR of the LN cathode is as large as 27.5 Ω cm² at 600°C, ~180 times larger than that of BSCF cathode (Supplementary information, Figs S1 and S3). However, the high electrical conductivity of LN thin film (~300 S cm^{-1})[21] makes it suitable for surface coating on BSCF considering the low electrical conductivity of BSCF (~40 S cm^{-1})[22].

Fabrication of the hierarchical shell onto BSCF scaffold. Fabrication of the hierarchical LN shell on BSCF is schematically shown in **Figures 1**. Before the microwave plasma treatment, a hierarchical LN precursor shell (porous) is fabricated by a two-step infiltration process. The substrate layer (untreated) is firstly obtained by infiltrating an aqueous solution of $La(NO_3)_3$ and $Ni(NO_3)_2$ (La:Ni=1:2 mole ratio) into the BSCF scaffold at a total metal ions concentration of 1.5 mol L^{-1} followed by heating at 850°C for 5 h to form BSCF-LN scaffold. The LN substrate coated on the BSCF scaffold is not dense at this stage. Consequently, citric acid (CA) was added to the aqueous solution at a molar ratio of 2:1 to the metal ions. The CA added solution was infiltrated into the BSCF-LN scaffold, and then heated at 850°C for 5 h again. The second LN layer with large pores was obtained on the LN substrate to form a hierarchical LN precursor shell. At this stage, the LN shell has not been densified. The sintering of the LN precursor shell cannot be realized by conventional heating process, because the densification temperature is over 1000°C, while phase reaction between BSCF and LN occurs at 900°C for only 30 min. The phase reaction is detrimental to the oxygen reduction reactivity (Supplementary information, Fig S4). This conflict can be circulated by using highly efficient microwave plasma treatment[23]. By treating the hierarchical LN precursor under microwave plasma at power of 500 W, the LN can be heated to 1800°C in a few seconds. The LN substrate is readily sintered to be dense in 10 min without new phase formation based on XRD (Supplementary information, Fig S4); meanwhile the second LN layer grows into cones on the substrate. Microwave-induced plasma is created in a quartz tube surrounded by a microwave cavity. Microwaves produced from a magnetron (a microwave generator) fill the cavity and cause the electrons in argon gas to oscillate. The oscillating electrons collide with other atoms in the flowing gas to create and maintain a high-temperature plasma. The target substance in microwave plasma can be heated by he collision of the oscillating electrons with the surface of the substance, so the heat is transferred from outside to inside. This allows the LN shell to be densified without phase reaction between

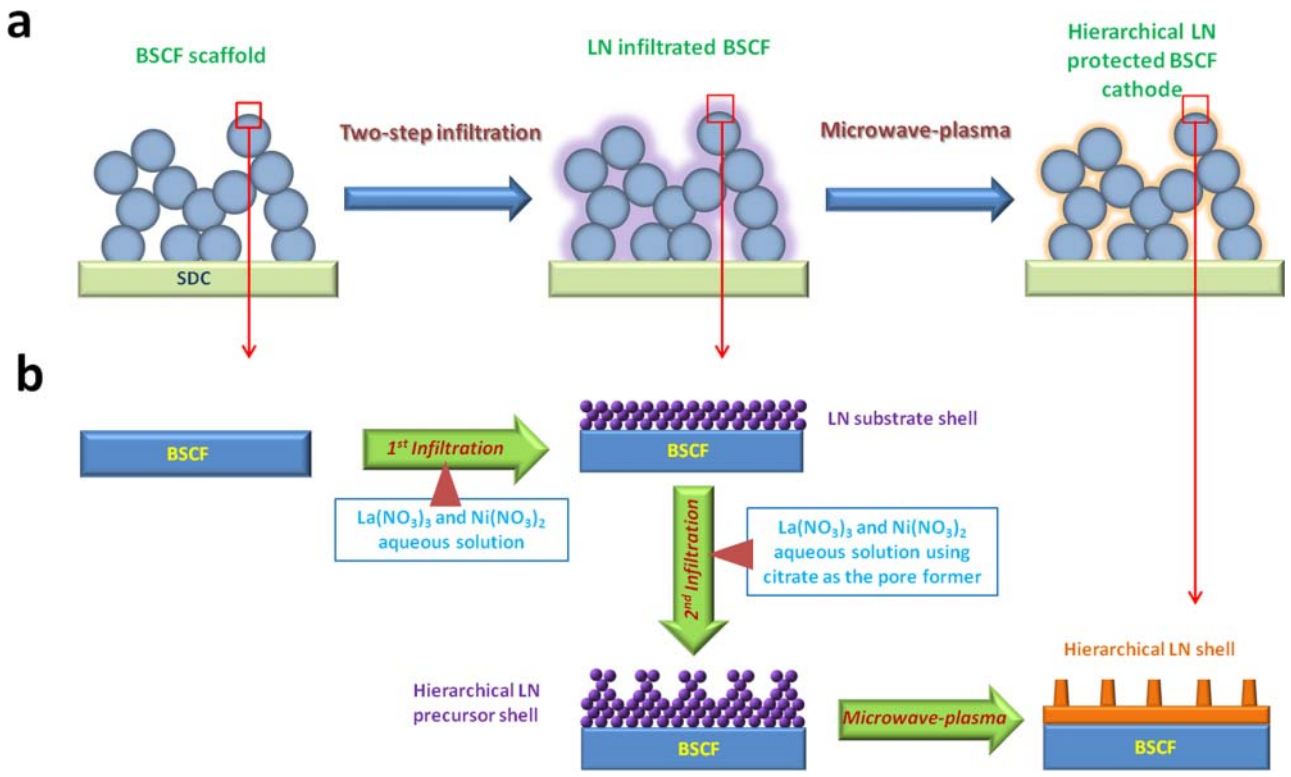

Figure 1 | Schamatic of preparation of the hierarchical LN shell protected BSCF cathode. (a) A two-step infiltration process is empolyed to introduce porous LN precursor shell onto the surface of BSCF scaffold and followed by microwave plasma treatment to obtain hierarcical LN shell. (b) In the 1st infiltration of the two-step infiltration process, $La(NO_3)_3$ and $Ni(NO_3)_2$ aqueous solution is infiltrated into BSCF scaffold. The LN substrate shell is obtained after heating at 850°C for 5 h. In order to obtained hierarcical LN precursor shell, ctrate added $La(NO_3)_3$ and $Ni(NO_3)_2$ aqueous is inflitrated and fired at 850°C for 5 h. Here the ctrate is used as the template to obtain bigger pores in the second LN shell. Finally, the microwave-plasma is used to heat the precurosr shell to make hierarchical LN shell.

LN and BSCF, if the heating time is elaborately controlled. A treatment of 30 min leads to the decreased ORR activity of the cathode, so the samples are treated for 10 min to prevent the undesired phase reaction in the present study.

Microstructure and CO_2 resistivity of the electrode. The morphology of the hierarchical LN is controlled by the LN loading amount in the second infiltration step (**Figure 2**). Without the second LN infiltration, only a 200–250 nm thick LN shell can be obtained (Figure 2b and Supplementary information, Fig S5). When the second LN infiltration loading amount reaches 6 wt% (total loading is 12 wt%), some dots with a diameter of 100 nm appear on the LN substrate. When the total loading amount is increased to 26wt%, the cones form on the substrate with a length of ~1 μm and diameter of ~100 nm (**Figure 2f**, Supplementary information, Fig S6).

We treated the hierarchical cathode in 10 vol% CO_2-containing air for 1 h at 600°C. The pristine BSCF and the BSCF-LN (before MP treatment) cathodes were also treated under the same conditions for comparison. CO_2-temperature programmed desorption (TPD) and FT-IR was performed to test their resistivity to CO_2. As shown in **Figure 3**, strong CO_2 desorption peak and adsorption at 1630, 1450, 1090, 1030 and 900 cm^{-1} attributing to the vibration bands for the CO_3^{2-} can be observed on the pristine BSCF after CO_2 treatment. Addition of LN can weaken the CO_2 poisoning effect dramatically. After microwave plasma treatment, the BSCF can be completely resistive to CO_2 under the protection of dense LN shell, this is evidenced by that no CO_2 desorption peak or vibration bands of CO_3^{2-} can be observed.

The electrochemical performance of the cathode was tested by AC impedance. The ASR of pristine BSCF is 0.162 Ω cm^2 at 600°C (**Figure 4a**). After LN infiltration heated at 850°C (before microwave plasma treatment), the ASR decreases to 0.078 Ω cm^2 at 600°C (**Figure 4b**). The improvement of the ORR is ascribed to increased three-phase boundary (TPB) between LN, BSCF and O_2. The sintering of the LN substrate (without LN cones) leads to the decrease of the oxygen reduction reactivity due to elimination of the TPB. Since the oxygen surface exchange rate on LN is lower than that on BSCF, the improvement of the exchange rate of the LN shell is realized by increasing the surface area (LN cones grow on LN substrate). The ASR reduces to 0.13 Ω cm^2 at 575°C.

The CO_2 resistivity of the cathodes is investigated in 10 vol%-CO_2 containing air. The ASR of the pristine BSCF increases to 20 times after introducing CO_2 into air in only 5 min. For LN infiltrated BSCF without microwave plasma treatment, the ASR increases to 2.4–3.8 times after 30 min and keep constant depending on the loading of the LN. With increasing LN loading, the CO_2 resistivity increases, but CO_2 poisoning effect cannot be completely eliminated due to the small void between LN grains. The microwave plasma treatment was thereby employed to sinter the LN shell. The ASR of the hierarchical cathode increases to 1.7 times of the original value after 1 h treatment in CO_2 and keeps constant for 24 h. The increase of the ASR is likely ascribed to the dilution of the air by CO_2, which can be supported by the factor that the ASR increases to about 1.4 times in 10 vol% Ar-containing air. Furthermore, by investigating the recovery of the ASR after removing CO_2, we also confirmed the complete CO_2 resistivity of the hierarchical cathode. It has been reported that CO_2 can not only be adsorbed onto the BSCF surface but also react with BSCF to form carbonates. Both cases will occupy the active sites for oxygen reduction, thus leading to the decreased ORR activity[24]. Although the adsorbed CO_2 can be removed after CO_2 treatment, the carbonates originating from reaction of CO_2 and BSCF are stable at 600°C. Therefore, the ASR cannot recover to the original value even after 24 h. As a comparison, the ASR of the hierarchical cathode recovers completely in only 51 min, indicating no carbonates form owing to the protection by the LN shell.

The fuel cell performance was also tested in 10 vol%-CO_2 containing air. Yan et al. reported that both open circuit voltages (OCVs) and power densities decreased after introduction of CO_2[25]. At 600°C, the power density decreased by ~58% in the presence of only 3.07 vol% CO_2 in air[25]. In the present study, both the OCVs and the power densities of the single fuel cell show similar values before and after introduction of CO_2 from 600 to 700°C (**Figure 5**). The slight decrease of power densities is ascribed to the dilution effect of the CO_2.

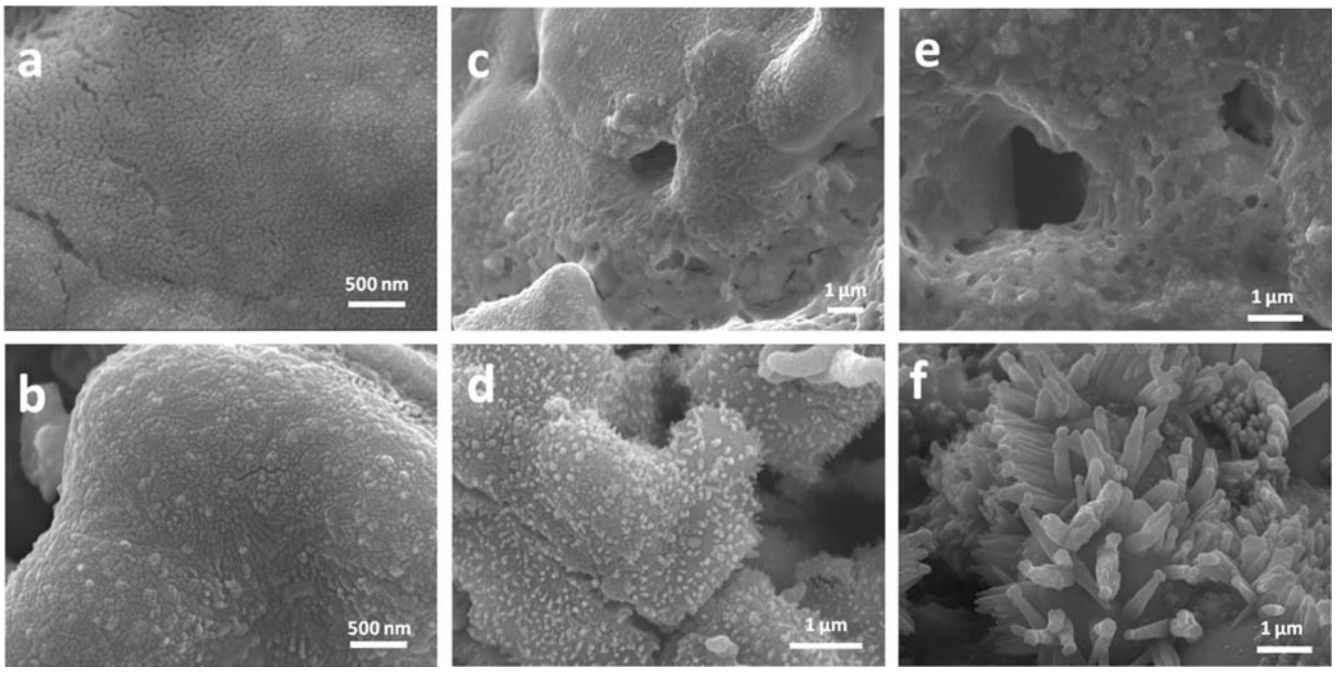

Figure 2 | SEM images of the LN shell on BSCF scaffold prepared in different conditions. The LN substrate shell with 6wt% LN loading before (a) and after (b) microwave plasma treatment. The hierarchical LN shell with 12 wt% LN loading before (c) and after (d) microwave plasma treatment. The hierarchical LN shell with 26 wt% LN loading (the second infiltration) before (e) and after (f) microwave plasma treatment.

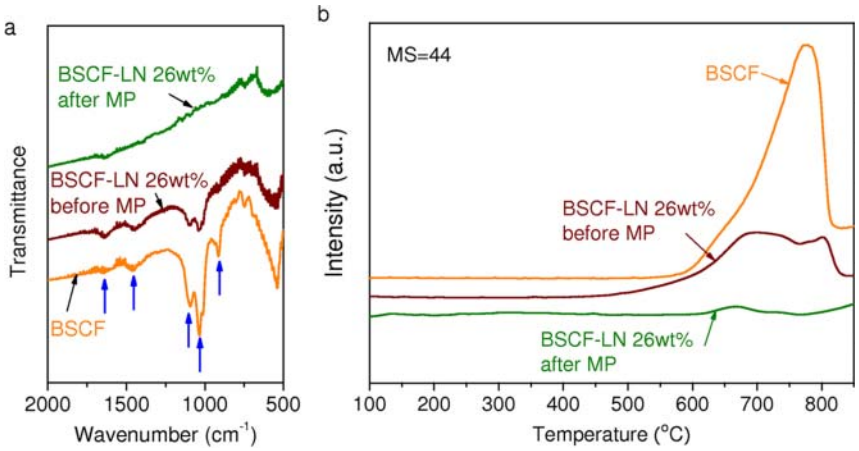

Figure 3 | CO_2 resistvity of the BSCF powders and the BSCF-LN powders with 26wt% LN loading before or after MP. The three types of powders were treated in air+10vol% CO_2 at 600°C for 1 h. (a) FT-IR spectra of the treated powders. The blue arrows indicates the vibrating peaks for carbonates. (b) CO_2-TPD of the treated powders. The peak area related to the amount of the carbonates.

Discussion

In the last decades, many efforts have been focused on lowering the operating temperature of SOFCs to intermediate range (500–700°C) without detriment of the fuel cell's generation efficiency. As drop the operating temperature to <650°C, the sluggish oxygen reduction reaction occurring on the cathode contribute the main potential loss in the fuel cell operation. In our previous study, a benchmark cathode- BSCF has been developed, which shows surprising high ORR activity reflected by its low area specific resistance (ASR<0.15 Ω cm^2) at 600°C[11]. However, BSCF is susceptible to CO_2 attack when

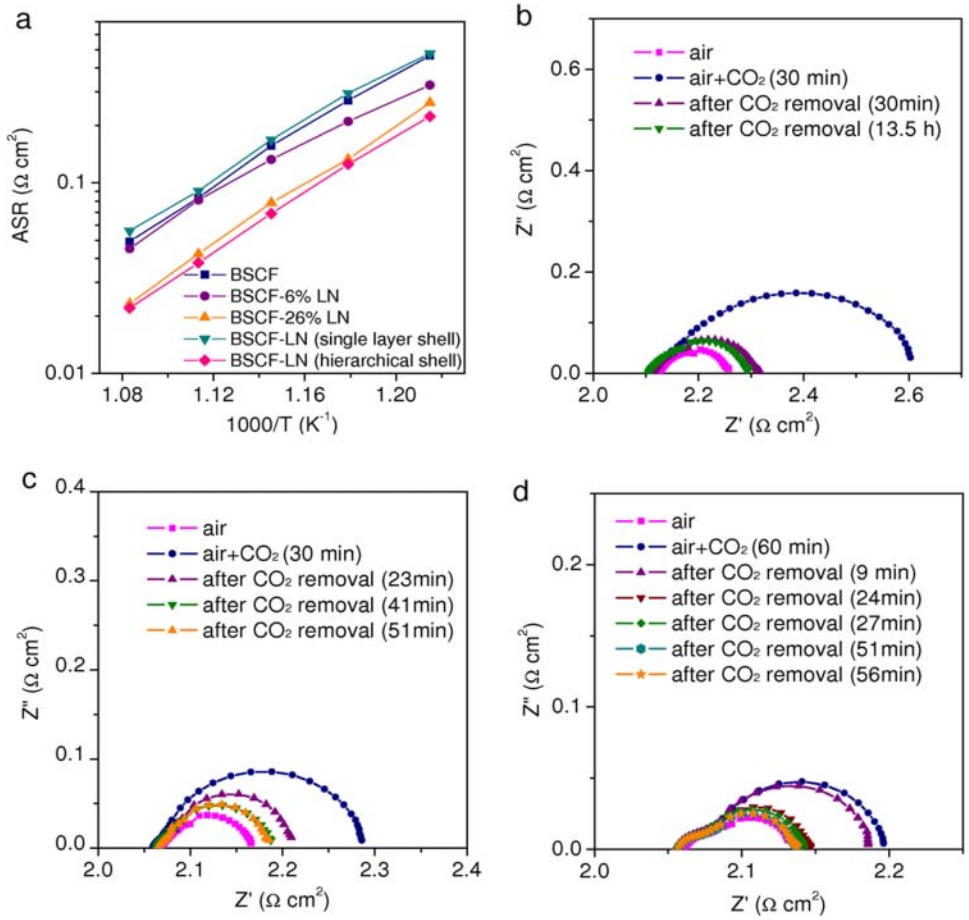

Figure 4 | Electrochemical analysis of the electrodes. (a) Arehnius plots of ASRs of the various electrodes based on the symmetric cells (BSCF-6%LN and BSCF-26%LN are the BSCF-LN cathodes before MP treatement). (b–d) The impedance spectroscopy of the electrode tested at 600°C in air, air+10vol% CO_2, and after removal of CO_2 from air. (b) 6wt% LN loading before microwave plasma treatment; (c) 26wt% LN loading before microwave plasma treatment; (d) 26wt% LN loading after microwave plasma treatment. The time in the bracket indicates the time after the introdtuction of CO_2 into air or after the remavol of the CO_2.

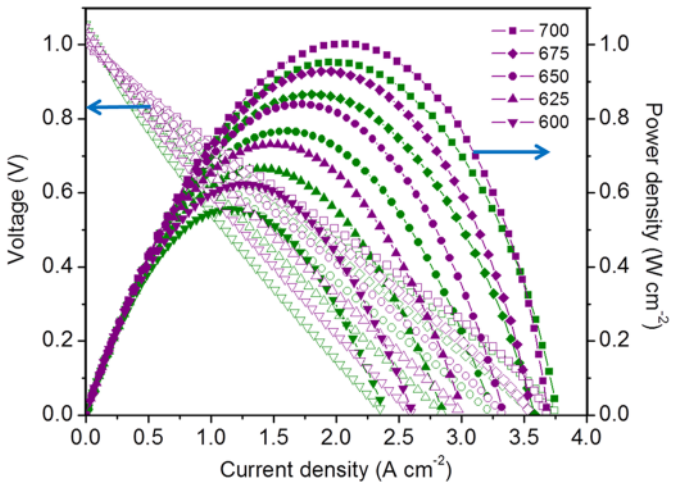

Figure 5 | Stability of the hierarchical LN protected BSCF cathode under working conditions. The cathode was prepared on a YSZ–Ni (50 : 50 vol%) anode supported SDC(5 μm)|YSZ(5 μm) electrolyte single cell. I–V and I–P curves of the single fuel cell were first tested using air in the cathode side at 600–700°C (purple curves). After introduction of 10 vol% CO_2 for 1 h, the fuel cell was tested again in CO_2 containing air (green curves).

temperature is decreased to 500–700°C, which is a vital problem blocking the BSCF's practical application[14–18]. Yan et al.[25] pointed out that the existence of ~0.2vol% of CO_2 in the oxidant gas can negatively affect the BSCF cathode performance. Since CO_2 is one of the components of the atmospheric air, the degradation of the BSCF cathode is inevitable when air is used as oxidant. It can be even worse when the BSCF cathode is used in a single chamber SOFC, which consists of only one gas chamber, wherein the anode and cathode are exposed to the same mixture of fuel and oxidant gas[26,27]. Since the hydrocarbons are used as the fuel in single chamber SOFCs, the CO_2 as a product of the anode reaction can reach a concentration of ~10vol% or higher in operation condition[28]. Besides BSCF, other high-performance cathodes like SSC are also susceptible to CO_2 attack. On the other hand, some oxides like LN exhibit good resistance to CO_2 impurity from 30 to 1000°C[29]. However, the electrochemical performance of the LN cathode is very poor below 700°C[30]. In our previous study, we have developed a novel cathode material $(La_{0.8}Sr_{0.2})_{0.95}Ag_{0.05}MnO_{3-\delta}$ showing tolerance to CO_2. However, the ORR activity of $(La_{0.8}Sr_{0.2})_{0.95}Ag_{0.05}MnO_{3-\delta}$ is also unsatisfied below 650°C[31]. It is a trade-off between ORR activity and CO_2 resistivity for the currently used cathodes. New generation cathodes are highly desirable to realize the full commercialization of SOFCs.

In order to solve the above mentioned problem, we have proposed that the infiltration technique may be used to fabricate a functional protecting layer on the currently used electrode materials to form a core-shell structured cathode[4]. However, the difficulty may lie in the densification of the protecting layer without phase reaction between the layer and the electrode material. Here, we successfully fabricate a hierarchical shell-covered porous cathode through infiltration followed by microwave plasma treatment. The high heating efficiency of microwave plasma allows the sintering of protecting layer in only few minutes, avoiding the phase reaction between LN and BSCF. With the protective shell, the BSCF based cathode can work stably in 10vol% of CO_2 containing atmosphere. Additionally, the hierarchical structure of the shell can also improve the ORR activity due to enlarged surface area. An ASR of as low as 0.13 Ω cm^2 has been achieved at 575°C, which is lower than that of the pristine BSCF cathode (0.27 Ω cm^2 as shown in **Figure 4a**) and other well-performing cathodes, e.g. SNC[12] and SSC[13]. It is worth of noting that the oxygen surface exchange coefficient of LN is 7.0×10^{-9} cm^{2}s^{-1} at 500°C, which is much lower than that of BSCF 1.1×10^{-6} cm^{2}s^{-1} at 500°C[32]. Further significant enhancement of ORR activity would be expected, if the material with high oxygen surface exchange coefficient is used as the shell.

In summary, the hierarchical LN shell was formed by microwave plasma treatment on the BSCF scaffold. The cathode showed high ORR activity and complete resistivity to CO_2 attack at intermediate temperature, thus may lead to the widespread application of IT fuel cells.

Methods

BSCF was synthesized by a combined EDTA-citrate complexing process. $Ba(NO_3)_2$ (99.99+%, Sigma-Aldrich), $Sr(NO_3)_2$ (99.99+%, Sigma-Aldrich), $Fe(NO_3)_3{\cdot}9H_2O$ (99.9+%, Sigma-Aldrich) and $Co(NO_3)_2{\cdot}6H_2O$ (99+%, Sigma-Aldrich) were used as the raw materials for metal sources. Stoichiometric amounts of these metal nitrates were mixed in deionized water and heated at 80°C. EDTA (99.9%, Sigma-Aldrich) and anhydrous citric acid (99.5%, Sigma-Aldrich) were then added as the complexing agents. The molar ratio of total metal nitrates, EDTA and citric acid in the solution was 1 : 1 : 2. To ensure complete complexation, solution pH was adjusted to 8 by adding NH_3 aqueous solution (28%). After evaporation of water at 150°C, a dark purple gel was recovered. The gel was pretreated on the furnace at 250°C for 8 hours to form a solid precursor. The solid precursor was then calcined at 900°C for 5 hours in air to obtain BSCF powders.

The BSCF powders were mixed with ethyl cellulose and terpinol to form slurry. The BSCF scaffold (porous BSCF layer) was prepared by tape casting the slurry onto both sides of a $Sm_{0.2}Ce_{0.8}O_{1.9}$ (SDC) disc followed by heating at 1000°C for 2 h. The average diameter of pores in BSCF scaffold is larger than 5 μm (supporting information, Figure S7), which facilitates the infiltration process. Infiltration was used to introduce LN precursor into BSCF scaffold. The hierarchical LN shell was obtained by treating the LN precursor under microwave plasma at power of 500 W for a few seconds.

The FT-IR spectra were collected with a Nicolet 6700 spectrometer by using KBr pellets in transmission mode. For CO_2 temperature programmed desorption (CO_2-TPD), approximately 100 mg of powders was loaded in a quartz tube. The tube was then placed in a tubular furnace equipped with a temperature controller. Argon at a flow rate of 20 mL min^{-1} under standard temperature and pressure (STP) was used as the carrier gas. The temperature was increased from 50 to 950°C at a ramp rate of 10°C min^{-1}. The effluent gases were monitored by a mass spectrometer (MS Hiden, Warrington, UK, QIC-20). The morphology of the electrode was studied by FESEM (JEOL 7001).

The electrochemical impedance spectra (EIS) of the symmetric cells were obtained using an Autolab, PGSTAT30 electrochemical workstation. The frequency range was 0.01 Hz to 100 kHz and the signal amplitude was 10 mV under open cell voltage conditions. The coin-shaped fuel cell was mounted onto an alumina tube and sealed by ceramic paste at 150°C before heated for testing. H_2 was fed into the anode side as a fuel at a flow rate of 60 ml min^{-1} (STP) while the cathode side was exposed to air. The current-voltage curves of the fuel cells operated between 600–700°C were obtained using an Autolab, PGSTAT30 electrochemical workstation.

1. Brett, D. J. L., Atkinson, A., Brandon, N. P. & Skinner, S. J. Intermediate temperature solid oxide fuel cells. *Chem. Soc. Rev.* **37**, 1568–1578 (2008).
2. Hibino, T. *et al.* A low-operating-temperature solid oxide fuel cell in hydrocarbon-air mixtures. *Science* **288**, 2031–2033 (2000).
3. Yang, L. *et al.* Enhanced sulfur and coking tolerance of a mixed ion conductor for SOFCs: $BaZr_{0.1}Ce_{0.7}Y_{0.2-x}Yb_xO_{3-\delta}$. *Science* **326**, 126–129 (2009).
4. Zhou, W. & Zhu, Z. H. The instability of solid oxide fuel cells in an intermediate temperature region. *Asia-Pac. J. Chem. Eng.* **6**, 199–203 (2011).
5. Steel, B. C. H. & Heinzel, A. Materials for fuel-cell technologies. *Nature* **414**, 345–352 (2001).
6. Jacobson, A. J. Materials for solid oxide fuel cells. *Chem. Mater.* **22**, 660–674 (2010).
7. Orera, A. & Slater, P. R. New chemical systems for solid oxide fuel cells. *Chem. Mater.* **22**, 675–690 (2010).
8. Tarancón, A., Burriel, M., Santiso, J., Skinner, S. J. & Kilner, J. A. Advances in layered oxide cathodes for intermediate temperature solid oxide fuel cells. *J. Mater. Chem.* **20**, 3799–3813 (2010).
9. Jiang, S. P. Development of lanthanum strontium manganite perovskite cathode materials of solid oxide fuel cells: a review. *J. Mater. Sci.* **43**, 6799–6833 (2008).
10. Peña, M. A. & Fierro, J. L. G. Chemical structures and performance of perovskite oxides. *Chem. Rev.* **101**, 1981–2018 (2001)
11. Shao, Z. P. & Haile, S. M. A high-performance cathode for the next generation of solid-oxide fuel cells. *Nature* **431**, 170–173 (2004).
12. Zhou, W., Shao, Z. P., Ran, R., Jin, W. Q. & Xu, N. P. A novel efficient oxide electrode for electrocatalytic oxygen reduction at 400–600°C. *Chem. Commun.* 5791–5793 (2008).
13. Zhou, W., Shao, Z. P., Ran, R. & Cai, R. Novel $SrSc_{0.2}Co_{0.8}O_{3-\delta}$ as a cathode material for low temperature solid-oxide fuel cell. *Electrochem. Commun.* **10**, 1647–1651 (2008).

14. Yi, J. X., Feng, S. J. Zuo, Y. B., Liu, W. & Chen, C. S. Oxygen Permeability and Stability of $Sr_{0.95}Co_{0.8}Fe_{0.2}O_{3-\delta}$ in a CO_2- and H_2O-Containing Atmosphere. *Chem. Mater.* **17**, 5856–5861 (2005).
15. Yi, J. X., Schroeder, M., Weirich, T. & Mayer, J. Behavior of $Ba(Co, Fe, Nb)O_{3-\delta}$ Perovskite in CO_2-Containing Atmospheres: Degradation Mechanism and Materials Design. *Chem. Mater.* **22**, 6246–6253 (2010).
16. Nadja, Z., Williamson, S. & Irvine, J.T.S., Elaboration of CO_2 tolerance limits of $BaCe_{0.9}Y_{0.1}O_{3-\delta}$ electrolytes for fuel cells and other applications. *Solid State Ionics* **176**, 3019–3026 (2005).
17. Arnold, M., Wang, H. H. & Feldhoff, A. Influence of CO_2 on the oxygen permeation performance and the microstructure of perovskite-type $(Ba_{0.5}Sr_{0.5})(Co_{0.8}Fe_{0.2})O_{3-\delta}$ membranes. *J. Membr. Sci.* **293**, 44–52 (2007).
18. Yan, A. Y. *et al.* A temperature programmed desorption investigation on the interaction of $Ba_{0.5}Sr_{0.5}Co_{0.8}Fe_{0.2}O_{3-\delta}$ perovskite oxides with CO_2 in the absence and presence of H_2O and O_2. *Appl. Catal. B* **80**, 24–31 (2008).
19. Hammami, R., Batis, H. & Minot, C. Combined experimental and theoretical investigation of the CO_2 adsorption on $LaMnO_{3+y}$ perovskite oxide. *Surf. Sci.* **603**, 3057–3067 (2009).
20. Zhou, W. *et al.* LSCF Nanopowder from Cellulose–Glycine-Nitrate Process and its Application in Intermediate-Temperature Solid-Oxide Fuel Cells. *J. Am. Ceram. Soc.* **91**, 1155–1162 (2008).
21. Garcia, G., Burriel, M., Bonanos, N. & Santiso, J. Electrical Conductivity and Oxygen Exchange Kinetics of $La_2NiO_{4+\delta}$ Thin Films Grown by Chemical Vapor Deposition. *J. Electrochem. Soc.* **155**, P28–P32 (2008).
22. Zhou, W. *et al.* Barium- and strontium-enriched $(Ba_{0.5}Sr_{0.5})_{1+x}Co_{0.8}Fe_{0.2}O_{3-\delta}$ oxides as high-performance cathodes for intermediate-temperature solid-oxide fuel cells. *Acta Mater.* **56**, 2687–2698 (2008).
23. Zhou, W., Liang, F., Shao, Z., Chen, J. & Zhu, Z. Heterostructured electrode with concentration gradient shell for highly efficient oxygen reduction at low temperature. *Sci. Rep.* **1**, 155 (2011).
24. Yan, A. Y., Maragou, V., Arico, A., Cheng, M. J. & Tsiakaras, P. Investigationof a $Ba_{0.5}Sr_{0.5}Co_{0.8}Fe_{0.2}O_{3-\delta}$ based cathode SOFC II. The effect of CO_2 on the chemical stability. *Appl. Catal. B* **76** 320–327 (2007).
25. Yan, A. Y. Investigation of a $Ba_{0.5}Sr_{0.5}Co_{0.8}Fe_{0.2}O_{3-\delta}$ based cathode IT-SOFC: I. The effect of CO_2 on the cell performance. *Appl. Catal. B* **66**, 64–71 (2006).
26. Yano, M., Tomita, A., Sano, M. & Hibino, T. Recent advances in single-chamber solid oxide fuel cells: A review. *Solid State Ionics* **177**, 3351–3359 (2007).
27. Riess, I. On the single chamber solid oxide fuel cells. *J. Power Sources* **175**, 325–337 (2008).
28. Hao, Y. Recent advances in single-chamber fuel-cells: Experiment and modeling. *Solid State Ionics* **177**, 2013–2021 (2006).
29. Klande, T., Efimov, K., Cusenza, S., Becker, K.-D. & Feldhoff, A. Effect ofdoping,microstructure,and CO_2 on $La_2NiO_{4+\delta}$-based oxygen-transporting materials. *J. Solid State Chem.* **184**, 3310–3318 (2011).
30. Escudero, M. J., Aguadero, A., Alonso, J. A. & Daza, L. A kinetic study of oxygen reduction reaction on La_2NiO_4 cathodes by means of impedance spectroscopy. *J. Electroanaly. Chem.* **611**, 107–116 (2007).
31. Zhou, W. A new cathode for solid oxide fuel cells capable of *in situ*electrochemical regeneration. *J. Mater. Chem.* **21**, 15343–15351 (2011).
32. Tarancon, A., Burriel, M., Santiso, J., Skinner, S. J. & Kilner, J. A. Advances in layered oxide cathodes for intermediate temperature solid oxide fuel cells. *J. Mater. Chem.* **20**, 3799–3813 (2010).

Acknowledgements

Dr Wei Zhou acknowledges the support of an Australian Research Council (ARC) Discovery Project grant (DP1095089). Prof Zongping Shao acknowledges the support of "China National Funds to Distinguished Young Scientists" under contract No. 51025209.

Author contributions

W.Z. Z.P.S. and Z.H.Z. drafted and revised the manuscript, conceptualized the study. W.Z. and F.L.L. performed synthesis, characterizations and analyses.

Additional information

Supplementary information accompanies this paper at http://www.nature.com/scientificreports

Competing financial interests: The authors declare no competing financial interests.

License: This work is licensed under a Creative Commons Attribution-NonCommercial-ShareAlike 3.0 Unported License. To view a copy of this license, visit http://creativecommons.org/licenses/by-nc-sa/3.0/

How to cite this article: Zhou, W., Liang, F., Shao, Z. & Zhu, Z. Hierarchical CO_2-protective shell for highly efficient oxygen reduction reaction. *Sci. Rep.* **2**, 327; DOI:10.1038/srep00327 (2012).